REPORT DOCUMENTATION PAGE

Form Approved OMB NO. 0704-0188

1. REPORT DATE (DD-MM-YYYY)	2. REPORT TYPE	3. DATES COVERED (From - To)
	New Reprint	-

4. TITLE AND SUBTITLE
Turbulent Transport at High Reynolds Numbers in an Inertial Confinement Fusion Context

5a. CONTRACT NUMBER
W911NF-13-1-0249

5b. GRANT NUMBER

5c. PROGRAM ELEMENT NUMBER
611102

6. AUTHORS
J. Melvin, P. Rao, R. Kaufman, H. Lim, Y. Yu, J. Glimm, D. H. Sharp

5d. PROJECT NUMBER

5e. TASK NUMBER

5f. WORK UNIT NUMBER

7. PERFORMING ORGANIZATION NAMES AND ADDRESSES
Research Foundation of SUNY at Stony Brc
Office of Sponsored Programs

West Sayville, NY 11796 -3362

8. PERFORMING ORGANIZATION REPORT NUMBER

9. SPONSORING/MONITORING AGENCY NAME(S) AND ADDRESS (ES)
U.S. Army Research Office
P.O. Box 12211
Research Triangle Park, NC 27709-2211

10. SPONSOR/MONITOR'S ACRONYM(S)
ARO

11. SPONSOR/MONITOR'S REPORT NUMBER(S)
63848-MA.7

12. DISTRIBUTION AVAILIBILITY STATEMENT
Approved for public release; distribution is unlimited.

13. SUPPLEMENTARY NOTES
The views, opinions and/or findings contained in this report are those of the author(s) and should not contrued as an official Department of the Army position, policy or decision, unless so designated by other documentation.

14. ABSTRACT
Mix is a critical input to hydro simulations used in modeling chemical or nuclear reaction processes in fluids. It has been identified as a possible cause of performance degradation in inertial confinement fusion (ICF) targets. Mix contributes to numerical solution uncertainty through its dependence on turbulent transport coefficients, themselves uncertain and even controversial quantities. These coefficients are a central object of study in this paper, carried out in an Richtmyer–Meshkov unstable circular two-dimensional (2D) geometry suggested by an ICF design. We study a pre-turbulent regime and a fully developed regime. The former, at times between the first shock passage and

15. SUBJECT TERMS
computational fluid dynamics, hydrodynamics, large eddy simulation (LES),mixing, turbulence modeling, shocks

16. SECURITY CLASSIFICATION OF:			17. LIMITATION OF ABSTRACT	15. NUMBER OF PAGES	19a. NAME OF RESPONSIBLE PERSON
a. REPORT	b. ABSTRACT	c. THIS PAGE			James Glimm
UU	UU	UU	UU		19b. TELEPHONE NUMBER 631-632-8370

Report Title

Turbulent Transport at High Reynolds Numbers in an Inertial Confinement Fusion Context

ABSTRACT

Mix is a critical input to hydro simulations used in modeling chemical or nuclear reaction processes in fluids. It has been identified as a possible cause of performance degradation in inertial confinement fusion (ICF) targets. Mix contributes to numerical solution uncertainty through its dependence on turbulent transport coefficients, themselves uncertain and even controversial quantities. These coefficients are a central object of study in this paper, carried out in an Richtmyer–Meshkov unstable circular two-dimensional (2D) geometry suggested by an ICF design. We study a pre-turbulent regime and a fully developed regime. The former, at times between the first shock passage and reshock, is characterized by mixing in the form of interpenetrating but coherent fingers and the latter, at times after reshock, has fully developed turbulent structures. This paper focuses on the scaling of spatial averages of turbulence coefficients under mesh refinement and under variation of molecular viscosity [i.e., Reynolds number (Re)]. We find that the coefficients scale under mesh refinement with a power of spatial grid spacing derived from the Kolmogorov 2/3 law, especially after reshock. We document the dominance of turbulent over molecular transport and convergence of the turbulent transport coefficients in the infinite Re limit. The transport coefficients do not coincide for the pre- and post-reshock flow regimes, with significantly stronger transport coefficients after reshock.

REPORT DOCUMENTATION PAGE (SF298)
(Continuation Sheet)

Continuation for Block 13

ARO Report Number 63848.7-MA
Turbulent Transport at High Reynolds Numbers...

Block 13: Supplementary Note

Approved for public release; distribution is unlimited.

J. Melvin
Department of Applied Mathematics and Statistics, Stony Brook University, Stony Brook, NY 11794

P. Rao[1]
Department of Applied Mathematics and Statistics, Stony Brook University, Stony Brook, NY 11794
e-mail: prao@ams.sunysb.edu

R. Kaufman
Department of Applied Mathematics and Statistics, Stony Brook University, Stony Brook, NY 11794

H. Lim
Department of Applied Mathematics and Statistics, Stony Brook University, Stony Brook, NY 11794

Y. Yu
Department of Applied Mathematics and Statistics, Stony Brook University, Stony Brook, NY 11794

J. Glimm
Department of Applied Mathematics and Statistics, Stony Brook University, Stony Brook, NY 11794
e-mail: glimm@ams.sunysb.edu

D. H. Sharp
Los Alamos National Laboratory, Los Alamos, NM 87545
e-mail: dcso@lanl.gov

Turbulent Transport at High Reynolds Numbers in an Inertial Confinement Fusion Context

Mix is a critical input to hydro simulations used in modeling chemical or nuclear reaction processes in fluids. It has been identified as a possible cause of performance degradation in inertial confinement fusion (ICF) targets. Mix contributes to numerical solution uncertainty through its dependence on turbulent transport coefficients, themselves uncertain and even controversial quantities. These coefficients are a central object of study in this paper, carried out in an Richtmyer–Meshkov unstable circular two dimensional (2D) geometry suggested by an ICF design. We study a pre turbulent regime and a fully developed regime. The former, at times between the first shock passage and reshock, is characterized by mixing in the form of interpenetrating but coherent fingers and the latter, at times after reshock, has fully developed turbulent structures. This paper focuses on the scaling of spatial averages of turbulence coefficients under mesh refinement and under variation of molecular viscosity [i.e., Reynolds number (Re)]. We find that the coefficients scale under mesh refinement with a power of spatial grid spacing derived from the Kolmogorov 2/3 law, especially after reshock. We document the dominance of turbulent over molecular transport and convergence of the turbulent transport coefficients in the infinite Re limit. The transport coefficients do not coincide for the pre- and post reshock flow regimes, with significantly stronger transport coefficients after reshock. [DOI: 10.1115/1.4027382]

Keywords: computational fluid dynamics, hydrodynamics, large eddy simulation (LES), mixing, turbulence modeling, shocks

1 Introduction

Turbulence, starting with Re $\approx$ 2000 [1], profoundly alters the fluid state. Such flows show a large increase in fluid transport, known as turbulent transport. Mix (either molecular level mixing, or fine scale granularity of flow mixtures) can occur in the absence of turbulence. The rate of mixing however, is greatly enhanced by the presence of turbulence. Mix of reactive components can enhance reactions, while admixture of nonreactive constituents can retard it. Thus, we see the importance of turbulent mix to theories of turbulent combustion and turbulent nuclear reactive processes. We analyze flows having Re $\approx 3.5 \times 10^4$ and higher; the starting value is set somewhat arbitrarily from the Reynolds numbers achieved in laboratory experiments, cf. [2], of the Rayleigh–Taylor (RT) instability. The appeal to RT experiments is based on the strong sensitivity of the RT macroscopic observables, i.e., the overall mixing rates, to turbulent transport [3,4]. In addition, when analysis consists of quantities subject to numerical uncertainties and even controversies, comparison to experiment (validation) is an indispensable strategy. A simulation validation protocol based on these ideas is described in [5].

The purpose of this paper is to explore the dependence of turbulent transport parameters on mesh and Re, for a range of Re including ICF applications and a range of mesh which includes the finest three dimensional (3D) meshes currently feasible for a complex engineering problem of this nature. This study, with its multiple simulations and variation of parameters, is not practical to carry out in 3D and so we regard this two dimensional (2D) study as offering insight to possible future 3D simulations. In contrast to 3D turbulence, 2D turbulence has two conserved quantities (energy and enstrophy). The turbulent energy spectrum has two asymptotic scaling ranges, a classical Kolmogorov scaling $k^{-5/3}$ for intermediate wave numbers k and a specifically 2D scaling law k^{-3} driven by enstrophy for large k up to the dissipation range. This theory was presented in the classical arguments of Kraichnan [6] and observed in direct numerical simulations (DNS) of Boffetta [7]. The energy flows in opposite directions under these two cascades, with their associated flow length scales,

[1]Corresponding author.

Contributed by the Fluids Engineering Division of ASME for publication in the JOURNAL OF FLUIDS ENGINEERING. Manuscript received February 16, 2013; final manuscript received April 6, 2014; published online July 9, 2014. Assoc. Editor: Stuart Dalziel.

while the wave number for energy injection marks the division between them.

The context selected for this study is a Richtmyer Meshkov (RM) fluid instability in a circular geometry. Aside from its inter est as a classical hydrodynamic instability, this problem is sugges tive of scientific issues which arise in studies of ICF capsules. Three stages in an ICF implosion are subject to mix and resulting performance degradation. These are the (i) ablation stage (RT instability modified by mass transfer effects), (ii) shock passage through various capsule layers (RM instabilities), and (iii) decel eration stage, which leads to hot spot formation (RT instability). The role of mix in each of these stages is the subject of ongoing studies. The present study pertains to the second stage, shock pas sage, with a possible relevance to the other ICF mix stages.

We study two qualitatively different flow regimes, the pre and post reshock flows. The pre reshock regime is incipiently turbu lent and characterized by mixing at the level of interpenetrating but coherent fingers. The post reshock regime is characterized by fully developed turbulence and a proliferation of fine scale mixing.

In a high Re shock driven flow, molecules ionize and exhibit strong thermal coupling to the electron and radiation fields. For this reason, we consider a fluid with a plasmalike highly heat con ductive Prandtl number $\mathrm{Pr} = 10^{-4}$ and a Schmidt number $\mathrm{Sc} = 1$. These are laminar transport values. The primary purpose of this paper is to examine the corresponding turbulent transport coeffi cients. We define the high Re limit as molecular viscosity $\nu \to 0$ with fixed values for Sc and Pr. This theoretical definition yields a uniquely specified theoretical limit. To complete the specification of fluid transport input parameters, we set the (molecular level) isotropic viscosity to zero and introduce a Re dependent shear (anisotropic) kinematic viscosity $\nu = 5.13 \times 10^{-4}$ m^2/s for $\mathrm{Re} = 6 \times 10^5$. We use inverse scaling of ν with Re for other Reynolds numbers. The levels of mixing and the value of Re achieved in ICF processes is a subject of ongoing research, out side of the scope of this study. We study a series of mesh levels (Δx from 6.25×10^{-4} to 1.56×10^{-4} m) and Re values from $\mathrm{Re} = 3.5 \times 10^4$ to a finite mesh approximation of $\mathrm{Re} \approx \infty$ (obtained by setting the molecular viscosity to 0). We mention previous studies of the same problem [5,8]. The numerical study is based on the front tracking code FronTier [9,10] enhanced with an LES turbulence model (Germano and Moin's dynamic subgrid model [11,12]) and dynamic subgrid scale (SGS) terms. The tracking reduces excess numerical species diffusion.

The SGS terms are defined using filters and test filters. For each term we introduce a model or approximate form with a to be determined coefficient. The filters are convolution operators which average the numerical solution with approximate localiza tion. We choose a unit mesh block average for the filter. The test filter is one unit coarser in resolution; for this we choose a 2^D array of mesh blocks in D dimensional space. The basic idea expressed in Germano's identity [11] is that the differences between the SGS stresses at the test filter level and the filter level can be evaluated (due to cancellation) in terms of quantities defined at a mesh level and otherwise missing coefficients can be determined. This computable difference of stresses, known as the Leonard term [13], is denoted as L.

Suppressing some details [14], the SGS model cM is a vector quantity whose divergence appears in the RHS of the conservation law. It has the form $cM = c\Delta x^2 \rho |S| \nabla U$, where Δx is the mesh spacing, S is the strain rate matrix, and ∇U is a solution gradient. [In the various conservation laws, ∇U becomes the anisotropic (isotropic) part of the strain rate matrix for the anisotropic (iso tropic) turbulent flux, the temperature gradient multiplied by a specific heat for the thermal flux or the species concentration gra dient for species flux.] The dimensionless coefficient c is to be determined separately for each of the conservation equations; the rest of this expression is the model M.

Let M^{diff} denote the difference between the filter dependent models M^{filter} and $M^{\mathrm{testfilter}}$ for the SGS terms taken at the filter and test filter grid levels. Setting the difference in models (assumed to have a common coefficient) proportional to the differ ences of stresses L, we have the equation

$$L = cM^{\mathrm{diff}} \tag{1}$$

where the same coefficient c relates models to unclosed SGS terms at the filter and test filter levels. The key equation is then $c = L/M^{\mathrm{diff}}$. The kinematic turbulent transport coefficient χ_{turb} is given by

$$\chi_{\mathrm{turb}} = c\Delta x^2 |S| \tag{2}$$

with c dimensionless and S the strain rate matrix. Here χ_{turb} denotes one of the turbulent shear viscosity, turbulent bulk viscos ity, turbulent species diffusion, or turbulent thermal diffusion, in each case with a distinct value for c. The dimensions of χ_{turb} are $[\mathrm{l}^2/\mathrm{t}]$.

The form of the SGS model $M = \chi_{\mathrm{turb}} \rho \nabla U$ as a product of two first order spatial derivatives multiplied by Δx^2 suggests that spa tial averages of χ_{turb} should be governed by Kolmogorov's 2/3 law, scaling as $\Delta x^{4/3}$. We see this relation definitively after reshock and a weak association at best to this relation before reshock. The scaling holds not only for the velocity field but for the concentration and thermal fields as well.

In Sec. 2, we examine the turbulent energy spectrum for our simulations. In Sec. 3, we relate the scaling laws for spatial mean values (defined by a simple average over the mixing zone) of the turbulent transport coefficients to scaling laws for Kolmogorov spectra. Using the scaling laws, we study the mean values of the transport coefficients as $\Delta x \to 0$ and $\mathrm{Re} \approx \infty$. Contrasts are drawn between the singly shocked regime (before reshock), which is pre turbulent and the doubly shocked, post reshock regime with fully developed turbulence. Conclusions are discussed in Sec. 4.

2 Scaling Laws for Primitive Equation Quantities

To examine the scaling properties of the turbulent spectral energy, we plot in Fig. 1 log log graphs of the turbulent energy spectrum $E(k)$ versus wave number k for the $\mathrm{Re} \approx \infty$ data taken from the finest simulation performed. The spectral analysis depends on a Fourier expansion. In view of the annulus shape of the mixing zone, we analyze with the approximate bounding box for the mixing zone. This results in a wave number normalized by size of the bounding box around the mixing zone (approximately 3/8 of the domain size). The left frame shows data from before reshock and the right frame after reshock. In the left frame we see a small wave number spectral range for $k^{-5/3}$ and beyond this, a steeper decay less than the theoretical value of 3 but possibly influenced by this effect. The turbulence in the left frame is not yet fully developed at this time and thus the flow features are out side of the scope of Kraichnan's theory. This imperfect scaling can also be observed in Table 1. In the right frame (after reshock), Fig. 1 suggests two scaling regimes, an approximate $k^{-5/3}$ and an approximate k^{-3}, which is consistent with Kraichnan's theory. This change in scaling law can also be observed in Table 2 with grid levels I II showing better agreement with each other than with grid level III. The Kolmogorov scale for the flows we com pute varies from microns or less to tens of microns at the time of reshock, while the finest mesh considered is $\Delta x = 1.56 \times 10^{-4}$ m. The possible k^{-3} scaling regime is visible for only 1/2 an order of magnitude in wave numbers and thus is not definitive, which is in line with comments from [7]. Beyond the differences in physical modeling between [7] and the present work, we do not come close to resolving the Kolmogorov scale. For a compressible calcula tion, we are not remotely near to DNS. Our finest mesh spacing $\Delta x = 1.56 \times 10^{-4}$ m is about a factor of 100 larger than our esti mated Kolmogorov scale $\eta \sim L \cdot \mathrm{Re}^{-3/4} \sim 2.5 \times 10^{-6}$ m, based on the length $L = 5.5 \times 10^{-2}$ m (width of the mixing zone) and

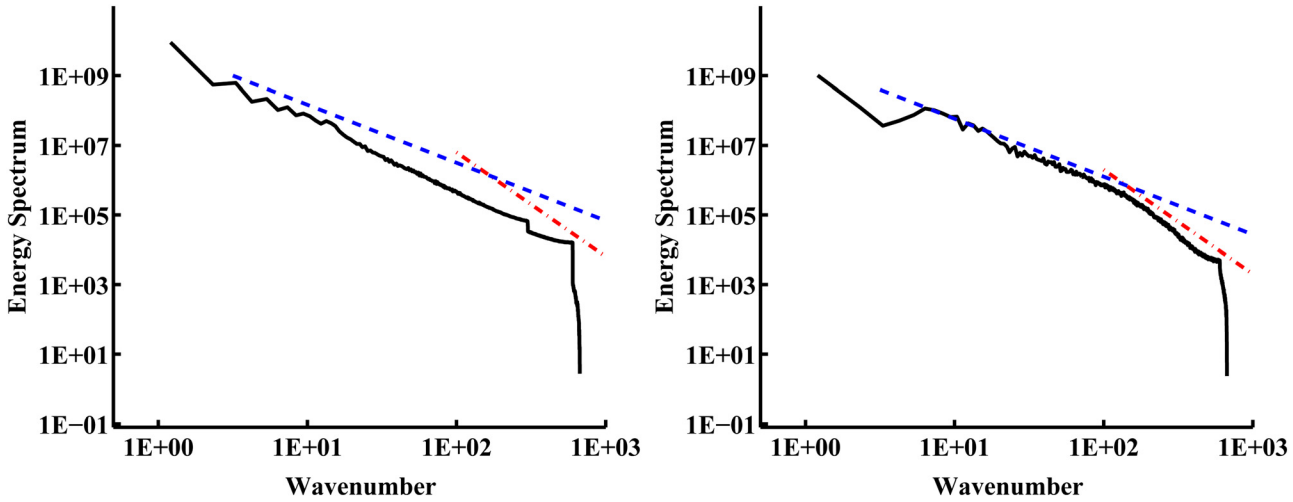

Fig. 1 Log-log energy spectrum plots versus wave number. The reference lines have slopes $k^{-5/3}$ (dashed) and k^{-3} (dashed-dotted). Left: Pre-reshock. Right: Post-reshock.

Table 1 Scaled mean turbulent transport coefficients. Mesh I: 400×800, with mesh II doubled and mesh III doubled again. Units are m^2/s before scaling. Time t 5.8×10^{-5}s, midway between the first and second shock passage. In the column Re ≈ ∞, the value is obtained by setting the molecular viscosity to 0.

Mesh	Re 3.5×10^4	Re 6×10^5	Re 6×10^6	Re 6×10^7	Re ≈ ∞
	cS' $\nu^a_{\text{turb}}/\Delta x^{4/3}$ scaled anisotropic turbulent viscosity ($m^{2/3}/s$)				
I	23	24	24	24	24
II	19	20	20	20	21
III	14	14	14	16	15
	$cS^{ti}_{\text{turb}}/\Delta x^{4/3}$ scaled isotropic turbulent viscosity ($m^{2/3}/s$)				
I	86	102	95	77	87
II	65	81	75	65	64
III	51	62	60	54	50
	cS' $\mu_{\text{turb}}/\Delta x^{4/3}$ scaled species turbulent diffusion ($m^{2/3}/s$)				
I	37	52	49	38	42
II	29	39	37	29	28
III	21	26	28	23	20
	cS' $\alpha_{\text{turb}}/\Delta x^{4/3}$ scaled turbulent thermal diffusion ($m^{2/3}/s$)				
I	103	71	44	40	47
II	65	66	42	33	34
III	30	56	41	33	28

Table 2 Scaled mean turbulent transport coefficients. Meshes and units as in Table 1. Time $t = 9.0 \times 10^{-5}$ s, shortly after the passage of reshock. In the column Re ≈ ∞, the value is obtained by setting the molecular viscosity to 0.

Mesh	Re 3.5×10^4	Re 6×10^5	Re 6×10^6	Re 6×10^7	Re ≈ ∞
	cS' $\nu^a_{\text{turb}}/\Delta x^{4/3}$ scaled anisotropic turbulent viscosity ($m^{2/3}/s$)				
I	44	51	53	47	54
II	48	48	56	58	53
III	57	49	64	64	62
	cS' $\nu^i_{\text{turb}}/\Delta x^{4/3}$ scaled isotropic turbulent viscosity ($m^{2/3}/s$)				
I	214	248	238	214	234
II	222	236	234	232	235
III	253	233	276	277	260
	cS' $\mu_{\text{turb}}/\Delta x^{4/3}$ scaled species turbulent diffusion ($m^{2/3}/s$)				
I	112	136	127	127	124
II	115	133	128	122	124
III	133	122	149	148	133
	cS' $\alpha_{\text{turb}}/\Delta x^{4/3}$ scaled turbulent thermal diffusion ($m^{2/3}/s$)				
I	126	163	143	122	132
II	106	181	158	135	145
III	103	174	191	174	149

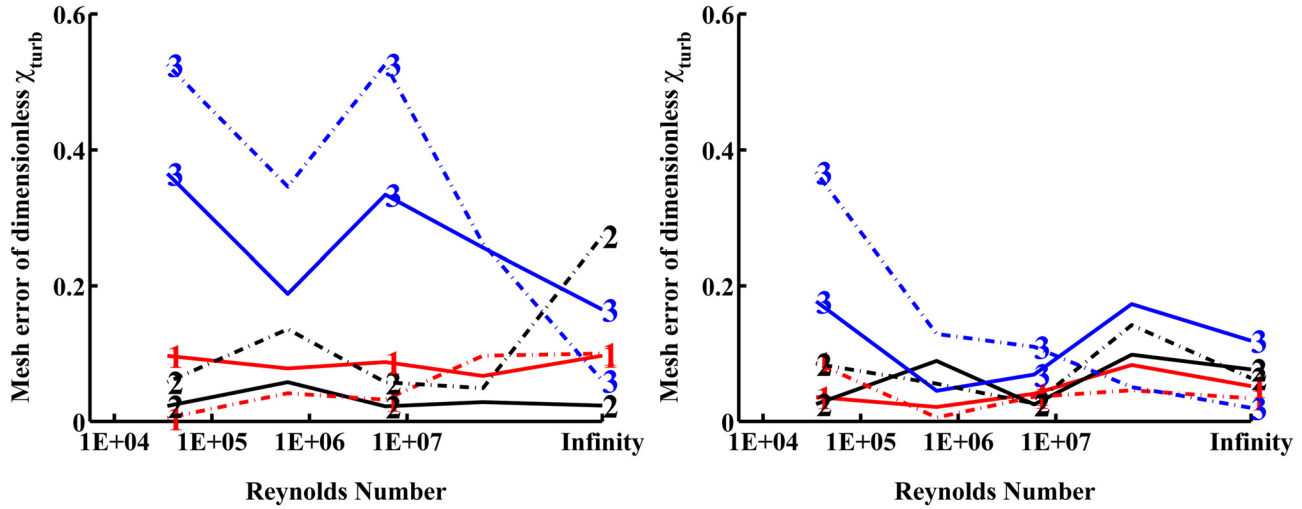

Fig. 2 Fractional mesh error for dimensionless turbulent transport coefficients, comparing coarse to fine (I–III) and medium to fine (II–III) grids, plotted versus Re. Left: Before reshock. Right: After reshock. Curves labeled 1, 2, 3 denote inverse isotropic viscosity, Schmidt number, and Prandtl number, respectively. The dashed-dotted line denotes the error in the comparison I–III and the solid line denotes the error in the comparison II–III.

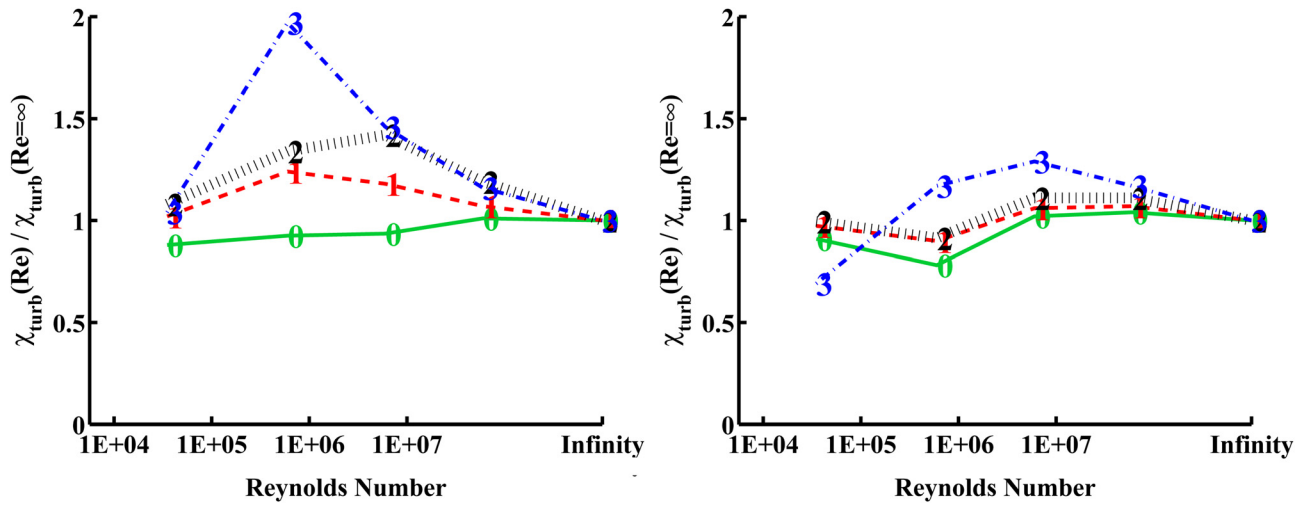

Fig. 3 Re dependence of mean turbulent transport coefficients for a Richtmyer–Meshkov instability. Fractional variation for each of the four-dimensional transport coefficients, plotted as $\chi_{turb}(Re)/\chi_{turb}(Re \approx \infty)$ versus Re, using the finest grid level. Left: Before reshock. Right: After reshock. Curves labeled 0, 1, 2, 3 denote anisotropic viscosity, isotropic viscosity, species diffusivity, and thermal diffusivity shown as a fraction of the values of these parameters at $Re \approx \infty$ and plotted versus the Reynolds number.

$\mathrm{Re} = 600,000$. This simple analysis suggests many unexplored length scales between the mesh resolution and the Kolmogorov scale, a statement which remains true even for the smallest $\mathrm{Re}(\mathrm{Re} = 35,000)$ considered here.

The statistical nature of the space time dependent pdfs varies as the distinct scaling ranges (intermediate, large k, dissipation range) change. Thus, mesh convergence requires that the coarse graining length scale [15 18] used to define the pdfs must be cho sen to lie within a single scaling range (if the mesh is chosen finer, i.e., not in this range, as with $\Delta x \to 0$).

3 Convergence and Variation of Mean Turbulent Transport Coefficients

Assuming that c is mesh convergent, the turbulent transport coefficient χ_{turb} defined by (2) cannot be asymptotically independ ent of Δx. The strain rate matrix S is assumed to satisfy the Kolmogorov 2/3 law for the local behavior of the two point corre lations, leading to a bound proportional to $\Delta x^{-2/3}$ for each deriva tive and for each turbulent transport term, and $\Delta x^{-4/3}$ for S factors combined with the gradient, part of M in the flux term. We rewrite (2) to obtain

$$\chi_{turb} = c\Delta x^{4/3}\left(S\Delta x^{2/3}\right) = c\Delta x^{4/3}S' \tag{3}$$

where (3) defines S'. Since c is assumed to converge to a finite limit as $\Delta x \to 0$ and S' is assumed to be bounded due to a Kolmo gorov type scaling law, we see that χ_{turb} vanishes with Δx at a pre dicted rate. Remarkably, we observe the same decay rate for all of the turbulent coefficients, even though the decay law is derived from an incompressible, velocity correlation decay (the Kolmo gorov 2/3 law for the decay of the velocity correlations). This scaling law is supported for the fully developed turbulence of Table 2 and is marginal at best for Table 1. It is clear that these

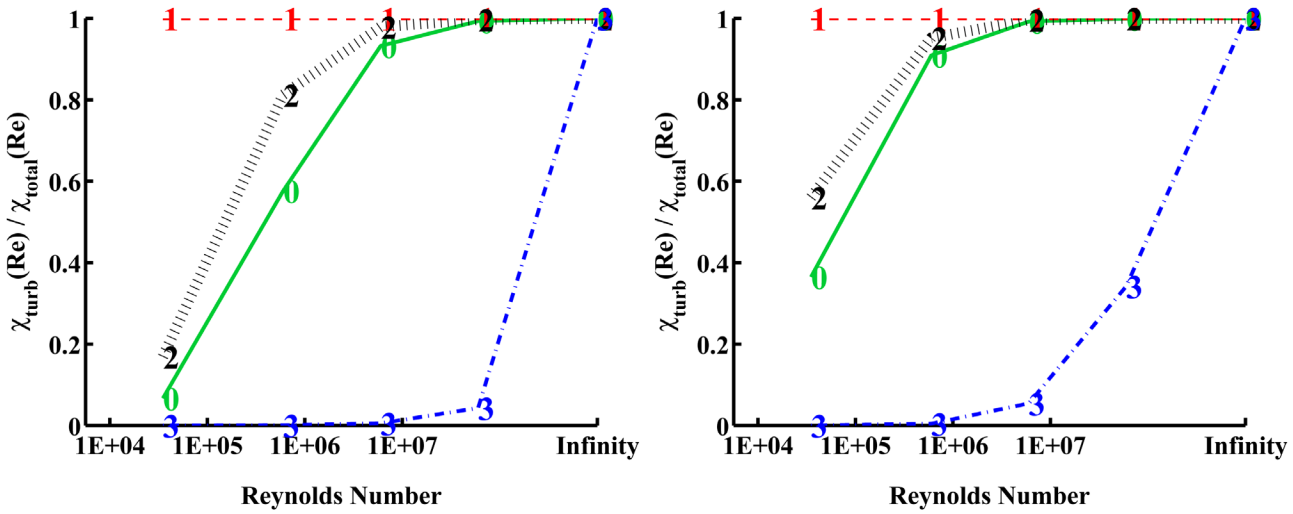

Fig. 4 Turbulent transport as a fraction of total transport plotted versus Re for each of four mean transport coefficients, with data taken at the fine grid level. Left: Before reshock. Right: After reshock. Curves labeled 0, 1, 2, 3 denote anisotropic viscosity, isotropic viscosity, species diffusivity, and thermal diffusivity, respectively, as a fraction of total transport.

two flow regimes, even in the infinite Re limit, define qualitatively different turbulent flows. Additionally, the post reshock coefficient mean values show only mild finite Re effects for $Re \geq 3.5 \times 10^4$, while the pre reshock coefficients transition to (different) nearly Re independent values at higher values of Re. The turbulent thermal and species coefficients are nearly identical to each other.

In Fig. 2, we plot fractional mesh errors versus Re, comparing coarse to fine and medium to fine, for the three dimensionless mean turbulent transport coefficients. The formula used for calculation of this error is $|f \quad l|/|f|$, where f stands for the mean turbulent dimensionless coefficient computed at the finest grid and l stands for the corresponding parameter at a medium/coarse grid level. We see that the mesh errors are either small in relative terms or convergent under mesh refinement or both for all values of Re. There is an exception for the turbulent Prandtl number and high Re turbulent Schmidt number, especially before reshock, for which further mesh refinement studies would be helpful. Further levels of mesh refinement would allow a deeper examination of 2D turbulence scaling properties for the present problem.

To better understand the high Re asymptotics, we plot in Fig. 3 the fractional change $\chi_{turb}(Re)/\chi_{turb}(Re \approx \infty)$ in the mean dimensional transport coefficients versus Re at the finest grid. The differences between the pre and post reshock turbulent flow can be seen by comparing the left frame to the right. We observe a rather mild Re dependence, especially for the fully developed turbulent flow (right).

To see the dominance of the turbulent transport as a fraction of the total transport, we plot χ_{turb}/χ_{total} versus Re in Fig. 4. Aside from the Prandtl number, the $Re \approx \infty$ values are nearly reached by $Re = 6 \times 10^6$ for the pre turbulent flow (left) and by $Re = 6 \times 10^5$ for fully turbulent flow (right). Note the striking qualitative difference between the Prandtl number and the other transport coefficients. Due to the very large level of laminar (molecular) heat conductivity assumed, even the high but finite $Re = 6 \times 10^7$ simulations display strong finite Re number effects for Pr_{total}. It is for this reason that the Prandtl number curves do not follow the pattern set by the other transport coefficients. The convergence of the total transport to its $Re \approx \infty$ asymptotic values is slower for the pre turbulent (singly shocked) flow than it is for the fully developed turbulent (doubly shocked) flow, a consequence of the smaller values of turbulent transport for the pre turbulent flow (singly shocked).

4 Conclusion

We have shown the mesh dependence for the spatially averaged turbulent transport coefficients to be either relatively small or convergent or both, for all values of Re considered and for the range of length scales (Δx) considered. The notion of pdf convergence depends on an observational length scale for coarse graining simulation values to define a local pdf. Convergence is limited to a range of length scales for which constant scaling behavior is valid. The post reshock coefficients have a mild Re dependence, while finite Re effects in these coefficients persist to higher Re values for the pre turbulent, single shocked case. The common post reshock Kolmogorov 2/3 law scaling among these coefficients is unexplained. The high level of thermal conductivity leads to finite Re effects in the thermal transport even for quite elevated values of Re.

Acknowledgment

This work is supported in part by Leland Stanford Junior University 2175022040367A (subaward with DOE as prime sponsor), Army Research Office W911NF0910306. Computational resources were provided by the Stony Brook Galaxy cluster and the Stony Brook/BNL New York Blue Gene/L IBM machine. This research used resources of the Argonne Leadership Computing Facility at Argonne National Laboratory, which is supported by the Office of Science of the U.S. Department of Energy under Contract DE AC02 06CH11357. David H. Sharp, Fellow Los Alamos National Laboratory, retired. Los Alamos National Laboratory preprint LA UR 13 20765. Stony Brook University preprint SUNYSB AMS 13 02.

References

[1] Dimotakis, P. E., 2000, "The Mixing Transition in Turbulent Flows," J. Fluid Mech., **409**, pp. 69–98.
[2] Smeeton, V. S., and Youngs, D. L., 1987, "Experimental Investigation of Turbulent Mixing by Rayleigh-Taylor Instability (Part 3)," AWE Report No. 035/87.
[3] Lim, H., Iwerks, J., Glimm, J., and Sharp, D. H., 2010, "Nonideal Rayleigh-Taylor Mixing," Proc. Natl. Acad. Sci. U.S.A., **107**(29), pp. 12786–12792.
[4] Lim, H., Iwerks, J., Yu, Y., Glimm, J., and Sharp, D. H., 2010, "Verification and Validation of a Method for the Simulation of Turbulent Mixing," Phys. Scr., **T142**, p. 014014.

[5] Melvin, J., Rao, P., Kaufman, R., Lim, H., Yu, Y., Glimm, J., and Sharp, D. H., 2013, "Atomic Scale Mixing for Inertial Confinement Fusion Associated Hydro Instabilities." High Energy Density Phys., **9**, pp. 288–298.
[6] Kraichnan, R. H., 1967, "Inertial Ranges in Two-Dimensional Turbulence," J. Fluid Mech., **16**, pp. 1417–1423.
[7] Boffetta, G., 2007, "Energy and Enstrophy Fluxes in the Double Cascade of Two-Dimensional Turbulence," J. Fluid Mech, **589**, pp. 253–260.
[8] Lim, H., Yu, Y., Glimm, J., Li, X. L., and Sharp, D. H., 2010, "Subgrid Models for Mass and Thermal Diffusion in Turbulent Mixing," Phys. Scr., **T142**, p. 014062.
[9] George, E., Glimm, J., Grove, J. W., Li, X.-L., Liu, Y.-J., Xu, Z.-L., and Zhao, N., 2003, "Simplification, Conservation and Adaptivity in the Front Tracking Method," *Hyperbolic Problems: Theory, Numerics, Applications*, T. Hou and E. Tadmor, Eds., Springer, Berlin, Germany, pp. 175–184.
[10] Bo, W., Liu, X., Glimm, J., and Li, X., 2011, "A Robust Front Tracking Method: Verification and Application to Simulation of the Primary Breakup of a Liquid Jet," SIAM J. Sci. Comput., **33**, pp. 1505–1524.
[11] Germano, M., Piomelli, U., Moin, P., and Cabot, W. H., 1991, "A Dynamic Subgrid Scale Eddy Viscosity Model," Phys. Fluids A, **3**, pp. 1760–1765.
[12] Moin, P., Squires, K., Cabot, W., and Lee, S., 1991, "A Dynamic Subgrid-Scale Model for Compressible Turbulence and Scalar Transport," Phys. Fluids A, **3**, pp. 2746–2757.
[13] Pope, S. B., 2000, *Turbulent Flows*, Cambridge University Press, Cambridge, NY.
[14] Ma, T., 2006, "Large Eddy Simulation Of Variable Density Flows," Ph.D. thesis, University of Maryland, College Park, MD.
[15] Kaman, T., Kaufman, R., Glimm, J., and Sharp, D. H., 2012, "Uncertainty Quantification for Turbulent Mixing Flows: Rayleigh-Taylor Instability," *Uncertainty Quantification in Scientific Computing*, A. Dienstfrey and R. Boisvert, Eds., Vol. 377 of IFIP Advances in Information and Communication Technology, Springer, New York, pp. 212–225.
[16] Kaman, T., Lim, H., Yu, Y., Wang, D., Hu, Y., Kim, J.-D., Li, Y., Wu, L., Glimm, J., Jiao, X., Li, X.-L., and Samulyak, R., 2011, "A Numerical Method for the Simulation of Turbulent Mixing and Its Basis in Mathematical Theory," *Lecture Notes on Numerical Methods for Hyperbolic Equations: Theory and Applications: Short Course Book*, CRC/Balkema, London, pp. 105–129.
[17] Kaufman, R., Kaman, T., Yu, Y., and Glimm, J., 2012, "Stochastic Convergence and the Software Tool W*," *Proceeding Book of International Conference to Honour Professor E. F. Toro*, CRC, Taylor and Francis Group, London, pp. 37–41.
[18] Lim, H., Kaman, T., Yu, Y., Mahadeo, V., Xu, Y., Zhang, H., Glimm, J., Dutta, S., Sharp, D. H., and Plohr, B., 2012, "A Mathematical Theory for LES Convergence," Acta Math. Sci., **32**, pp. 237–258.